

Benzoselenophenylpyridine platinum complexes: green versus red phosphorescence towards hybrid OLEDs

Alla Petrenko,^a Karolis Leitonas^b, Dmytro Volyniuk^b, Glib V. Baryshnikov,^{c,d} Sergey Belyakov,^a Boris F. Minaev,^d Hans Ågren,^{c,e} Hranush Durgaryan^b, Juozas Vidas Gražulevičius,^{*b} Pavel Arsenyan^{*a}

^a *Latvian Institute of Organic Synthesis, Aizkraukles 21, LV-1006, Riga, Latvia;*
e-mail: pavel@osi.lv

^b *Kaunas University of Technology, Department of Polymer Chemistry and Technology, Radvilenu pl. 19, LT-50254, Kaunas, Lithuania; e-mail: juozas.grazulevicius@ktu.lt*

^c *Division of Theoretical Chemistry and Biology, School of Engineering Sciences in Chemistry, Biotechnology and Health, KTH Royal Institute of Technology, 10691, Stockholm, Sweden*

^d *Department of Chemistry and Nanomaterials Science, Bohdan Khmelnytsky National University, 18031, Cherkasy, Ukraine*

^e *College of Chemistry and Chemical Engineering, Henan University, Kaifeng, Henan 475004, P. R. China*

Experimental Section

¹H, ¹³C, and ⁷⁷Se NMR spectra were recorded on a Bruker Avance Neo spectrometer at 400.0, 100, and 76 MHz, respectively, at 303 K in CDCl₃/TMS or DMSO-*d*₆ solution. The ¹H chemical shifts are given relative to TMS, ¹³C relative to chloroform or DMSO, and ⁷⁷Se relative to dimethyl selenide. Infrared (IR) spectra were recorded with a Prestige-21 FTIR spectrometer (Shimadzu, Kyoto, Japan). GC-MS spectra were recorded on an Agilent 7690 GC instrument with MSD. HRMS spectra were recorded on Waters Synapt GII Q-ToF UPLC/MS.

Synthesis

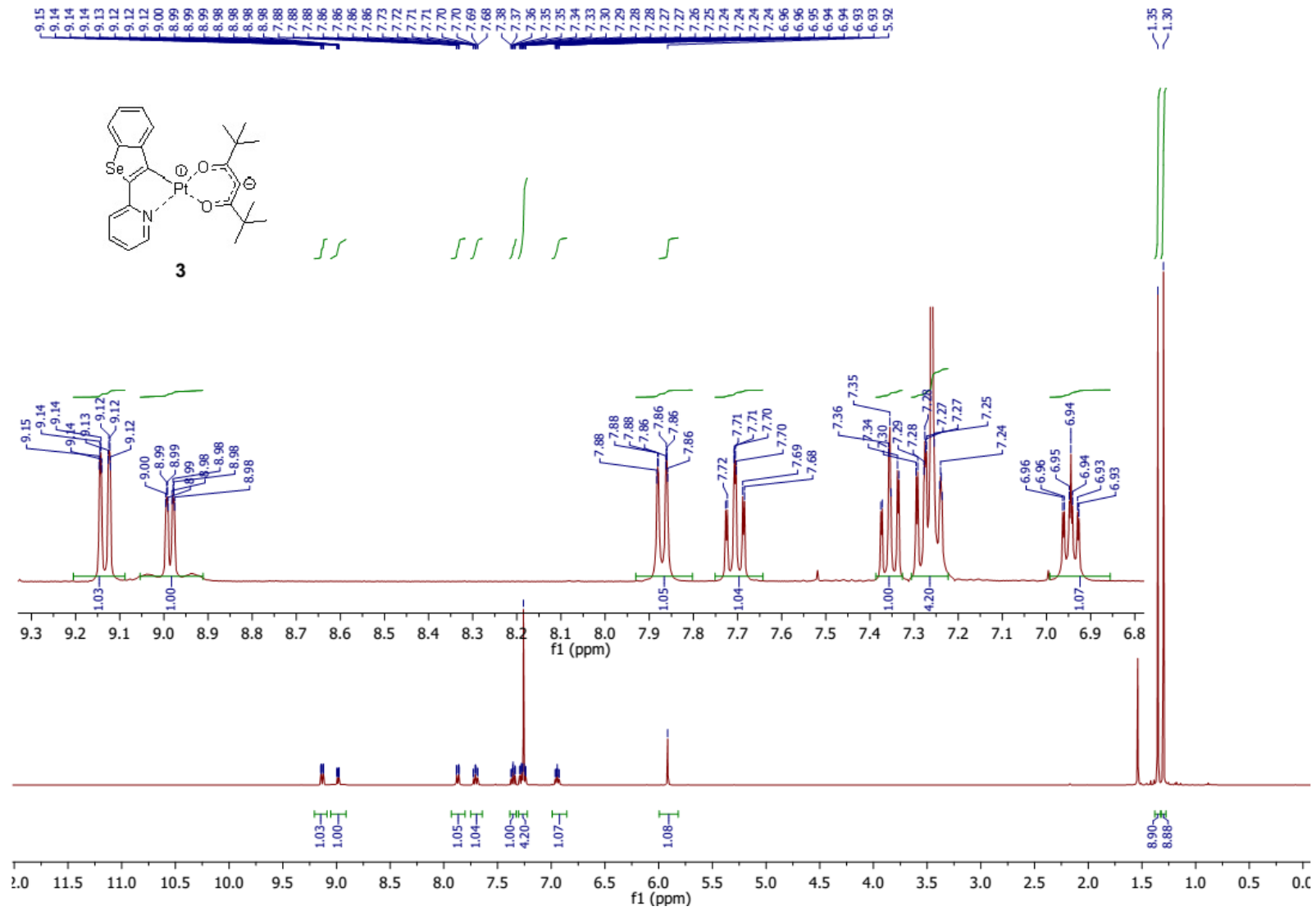
2-(Benzo[*b*]selenophen-3-yl)pyridine 4. To a solution of 3-iodobenzo[*b*]selenophene (2.5 g, 8.12 mmol), and 2-(trimethylstannyl)pyridine (2.35 g, 9.74 mmol) in dry xylene (25 ml) Pd(PPh₃)₄ (0.94 g, 0.81 mmol) and triphenylarsine (0.25 g, 0.81 mmol) were added. The resulting mixture was stirred at 110° C for 12 h. The progress of the reaction was followed by TLC. After cooling, the reaction mixture diluted with EtOAc, and filtered. The filtrate was washed with saturated aqueous NaCl solution, dried, and concentrated to give a crude oil. The oil was purified by silica gel chromatography (gradient 0-30% EtOAc, 0-30% CH₂Cl₂ in pet. Ether) to yield (1.64 g, 78%). ¹H NMR (400 MHz, Chloroform-*d*) δ 8.77 – 8.74 (m, 1H), 8.33 – 8.30 (m, 1H), 8.27 (s, 1H), 7.98 – 7.95 (m, 1H), 7.79 (td, *J* = 7.7, 1.8 Hz, 1H), 7.64 – 7.61 (m, 1H), 7.43 (ddd, *J* = 8.2, 7.2, 1.2 Hz, 1H), 7.37 – 7.33 (m, 1H), 7.29 (ddd, *J* = 7.7, 4.9, 1.2 Hz, 1H). ¹³C NMR (101 MHz, Chloroform-*d*) δ 156.0, 149.7, 142.4, 140.4, 139.7, 136.8, 129.6, 126.0, 125.9, 124.9, 124.9, 123.4, 122.2.

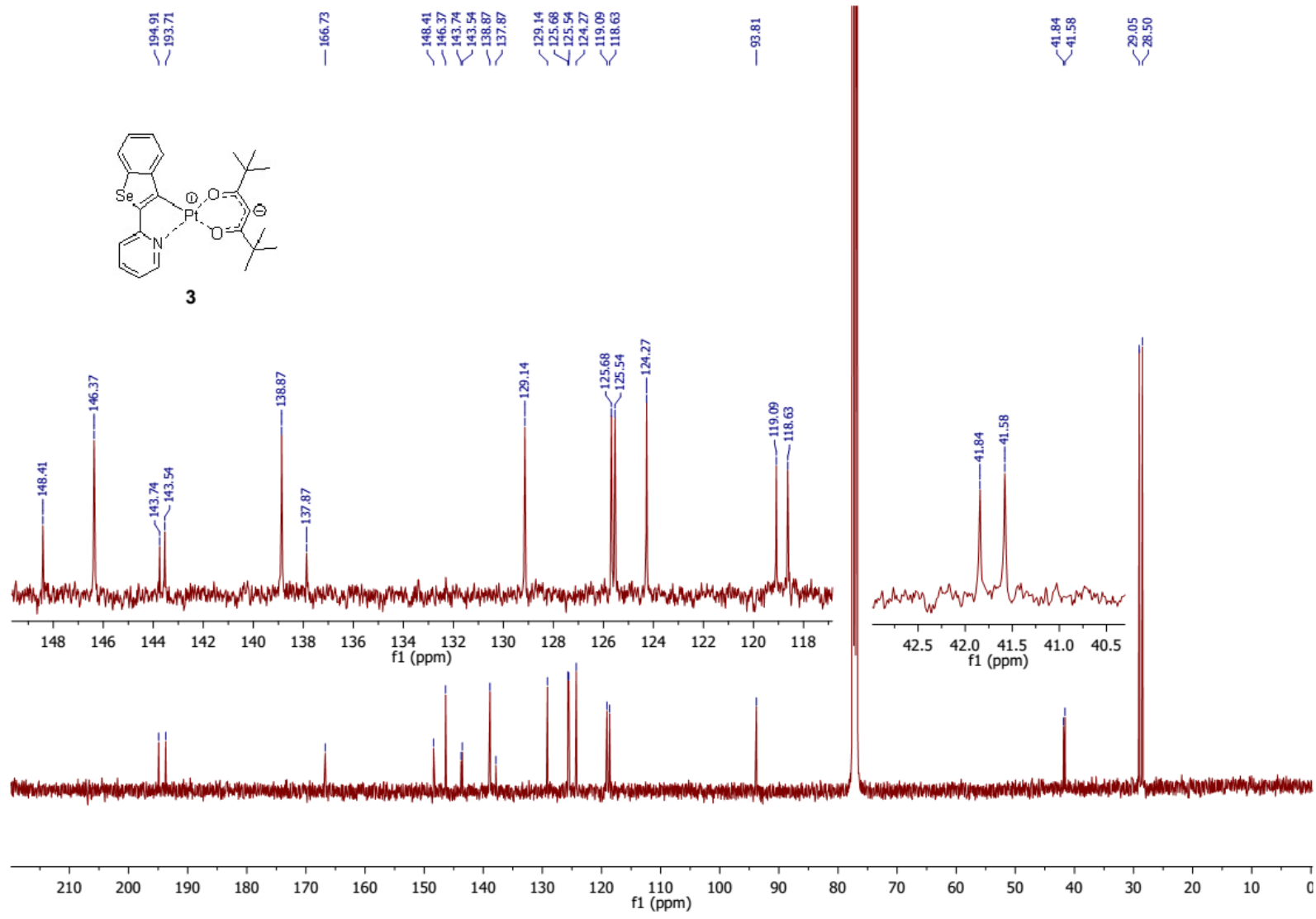
Complex 3: (a) Intermediate 2: To a mixture of **1** (233 mg, 0.9 mmol) in 2-methoxyethanol (20 mL) a solution of K₂PtCl₄ (150 mg, 0.36 mmol) in water (7 mL) was added, and the mixture was heated at 120 °C for 16 h under inert atmosphere. After cooling, 80 mL of water was added, and precipitates were collected by filtration. The precipitates was washed with methanol (15 mL) and hexane (20 mL) to afford **2** as a yellow solid 204 mg, (75%). ¹H NMR (400 MHz, Chloroform-*d*) δ 9.63 (ddd, *J* = 5.9, 1.6, 0.8 Hz, 1H), 9.34 (ddd, *J* = 5.9, 1.6, 0.8 Hz, 1H), 8.12 (d, *J* = 0.8 Hz, 1H), 8.07 (ddd, *J* = 8.2, 1.6, 0.8 Hz, 1H), 7.99 (ddd, *J* = 8.2, 7.4, 1.6 Hz, 1H), 7.86 – 7.81 (m, 1H), 7.81 – 7.73 (m, 2H), 7.72 (dp, *J* = 8.0, 0.7 Hz, 1H), 7.36 – 7.27 (m, 3H), 7.23 (ddd, *J* = 8.4, 7.2, 1.4 Hz, 1H), 7.10 (ddd, *J* = 8.0, 7.1, 1.3 Hz, 1H), 7.02 (ddd, *J* = 7.4, 5.9, 1.4 Hz, 1H), 6.87 (ddd, *J* =

8.3, 7.1, 1.2 Hz, 1H), 6.25 – 6.14 (m, 1H). HRMS (ESI): calcd for $C_{26}H_{17}ClN_2PtSe_2$ $[M-Cl]^+$ 711.9375, found 711.9380. (b) A mixture of **2** (100 mg, 0.13 mmol), 2,2,6,6-tetramethylheptane-3,5-dione (48 mg, 0.26 mmol), and Ag_2O (45 mg, 0.19 mmol) in 2-methoxyethanol (8 mL) was heated at 110°C for 30 h under inert atmosphere. After cooling, chloroform (100 mL) and water (50 mL) were added, and the mixture was vigorously shaken. The organic layer was separated, and the aqueous layer was extracted with chloroform (100 mL \times 2). The combined organic layers were washed with water (50 mL \times 2) and saturated aqueous NaCl solution (100 mL), and then dried over anhydrous Na_2SO_4 . Then volatiles were removed and the residue was purified by silica gel column chromatography (chloroform as eluent) to afford **3** as a yellow solid (75 mg, 91%). 1H NMR (400 MHz, Chloroform-*d*) δ 9.15 – 9.12 (m, 1H), 8.99 (ddd, $J = 5.8, 1.5, 0.8$ Hz, 1H), 7.89 – 7.85 (m, 1H), 7.73 – 7.68 (m, 1H), 7.35 (ddd, $J = 8.1, 7.0, 1.5$ Hz, 1H), 7.30 – 7.23 (m, 1H), 6.94 (ddd, $J = 7.4, 5.9, 1.5$ Hz, 1H), 5.92 (s, 1H), 1.35 (s, 9H), 1.30 (s, 1H). ^{13}C NMR (101 MHz, Chloroform-*d*) δ 194.9, 193.7, 166.7, 148.4, 146.4, 143.7, 143.5, 138.9, 137.9, 129.1, 125.7, 125.5, 124.3, 119.1, 118.6, 93.8, 41.8, 41.6, 29.0, 28.5. ^{77}Se NMR (76 MHz, Chloroform-*d*) δ 481.9. HRMS (ESI): calcd for $C_{20}H_{24}N_7PtSe$ $[M]^+$ 636.0855, found 636.0905. Elemental analysis calcd. for $C_{24}H_{27}NO_2PtSe$: C, 45.36; H, 4.28; N, 2.20; found: C, 45.11; H, 4.21; N, 2.14.

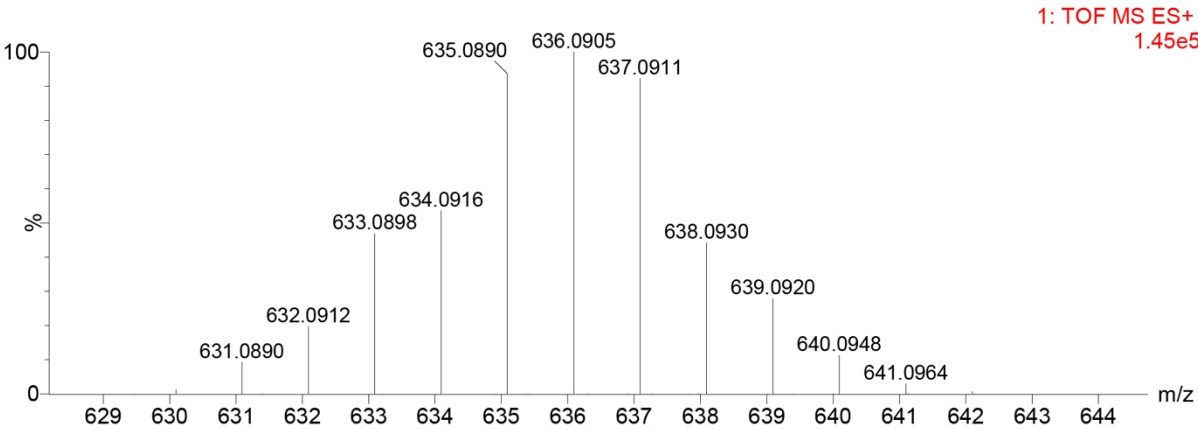
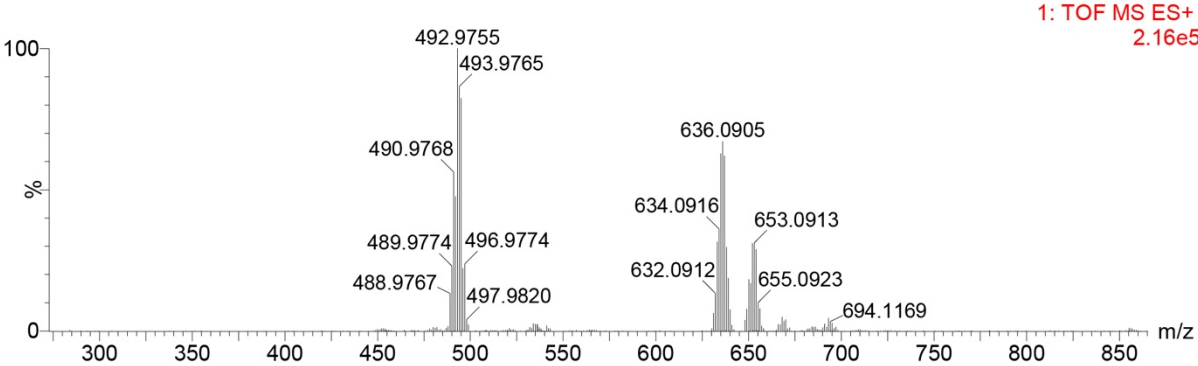
Complex **6**: (a) Intermediate **5**: To a mixture of **4** (233 mg, 0.9 mmol) in 2-methoxyethanol (20 mL) a solution of K_2PtCl_4 (150 mg, 0.36 mmol) in water (7 mL) was added, and the mixture was heated at 120 °C for 120 h under inert atmosphere. After cooling, 80 mL of water was added, and precipitates were collected by filtration. The precipitates were washed with methanol (15 mL) and hexane (20 mL) to afford **5** as a yellow solid 173 mg, (64 %). HRMS (ESI): $C_{26}H_{17}ClN_2PtSe_2$ $[M+H]^+$ 747.9060, found 747.8977. (b) A mixture of **5** (156 mg, 0.2 mmol), 2,2,6,6-tetramethylheptane-3,5-dione (70 mg, 0.41 mmol), and Ag_2O (70 mg, 0.31 mmol) in 2-methoxyethanol (16 mL) was heated at 110°C for 120 h under inert atmosphere. After cooling, chloroform (100 mL) and water (50 mL) were added, and the mixture was vigorously shaken. The organic layer was separated, and the aqueous layer was extracted with chloroform (100 mL \times 2). The combined organic layers were washed with water (50 mL \times 2) and saturated aqueous NaCl solution (100 mL), and then dried over anhydrous Na_2SO_4 . The solvent was removed under reduced pressure and the residue

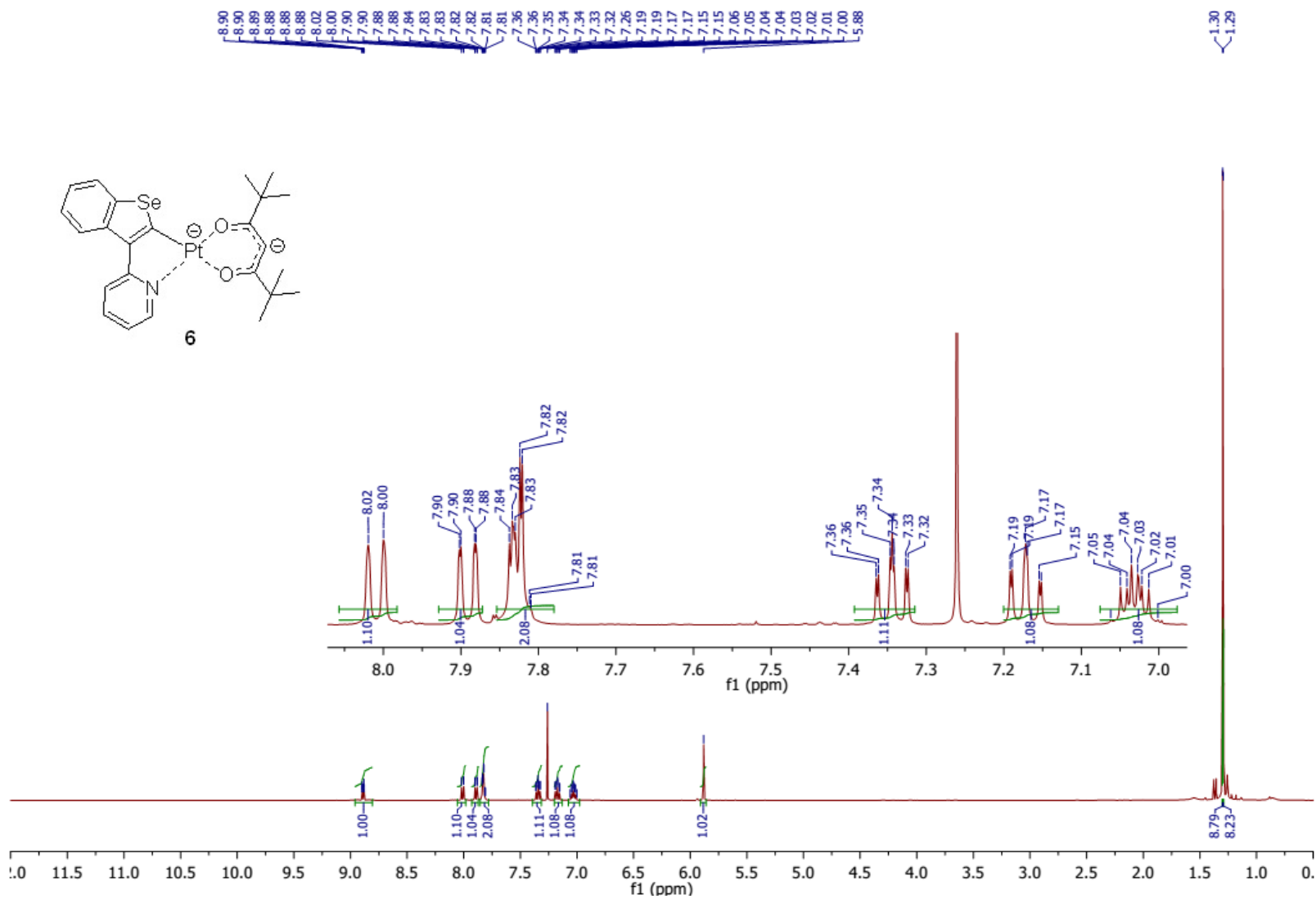
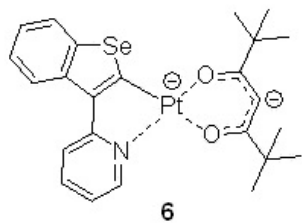
was purified by silica gel column chromatography (chloroform as eluent) to afford **6** as a yellow solid (23 mg, 18 %). ^1H NMR (400 MHz, Chloroform-*d*) δ 8.89 (dt, $J = 5.8, 1.3$ Hz, 1H), 8.01 (d, $J = 7.8$ Hz, 1H), 7.91 – 7.86 (m, 1H), 7.84 – 7.81 (m, 2H), 7.33 (ddd, $J = 8.2, 7.2, 1.3$ Hz, 1H), 7.17 (m, 1H), 7.06 – 7.01 (m, 1H), 5.88 (s, 1H), 1.30 (s, 9H), 1.29 (s, 1H). ^{13}C NMR (101 MHz, Chloroform-*d*) δ 195.5, 194.2, 165.1, 164.7, 147.7, 142.6, 139.4, 126.7, 124.6, 122.0, 120.2, 118.5, 117.8, 93.7, 41.7, 41.6, 28.7, 28.5. ^{77}Se NMR (76 MHz, Chloroform-*d*) δ 560.2. HRMS (ESI): calcd for $\text{C}_{20}\text{H}_{24}\text{N}_7\text{PtSe} [\text{M}]^+$ 636.0855, found 636.0889. Elemental analysis calcd. for $\text{C}_{24}\text{H}_{27}\text{NO}_2\text{PtSe}$: C, 45.36; H, 4.28; N, 2.20; found: C, 45.08; H, 4.34; N, 2.15.

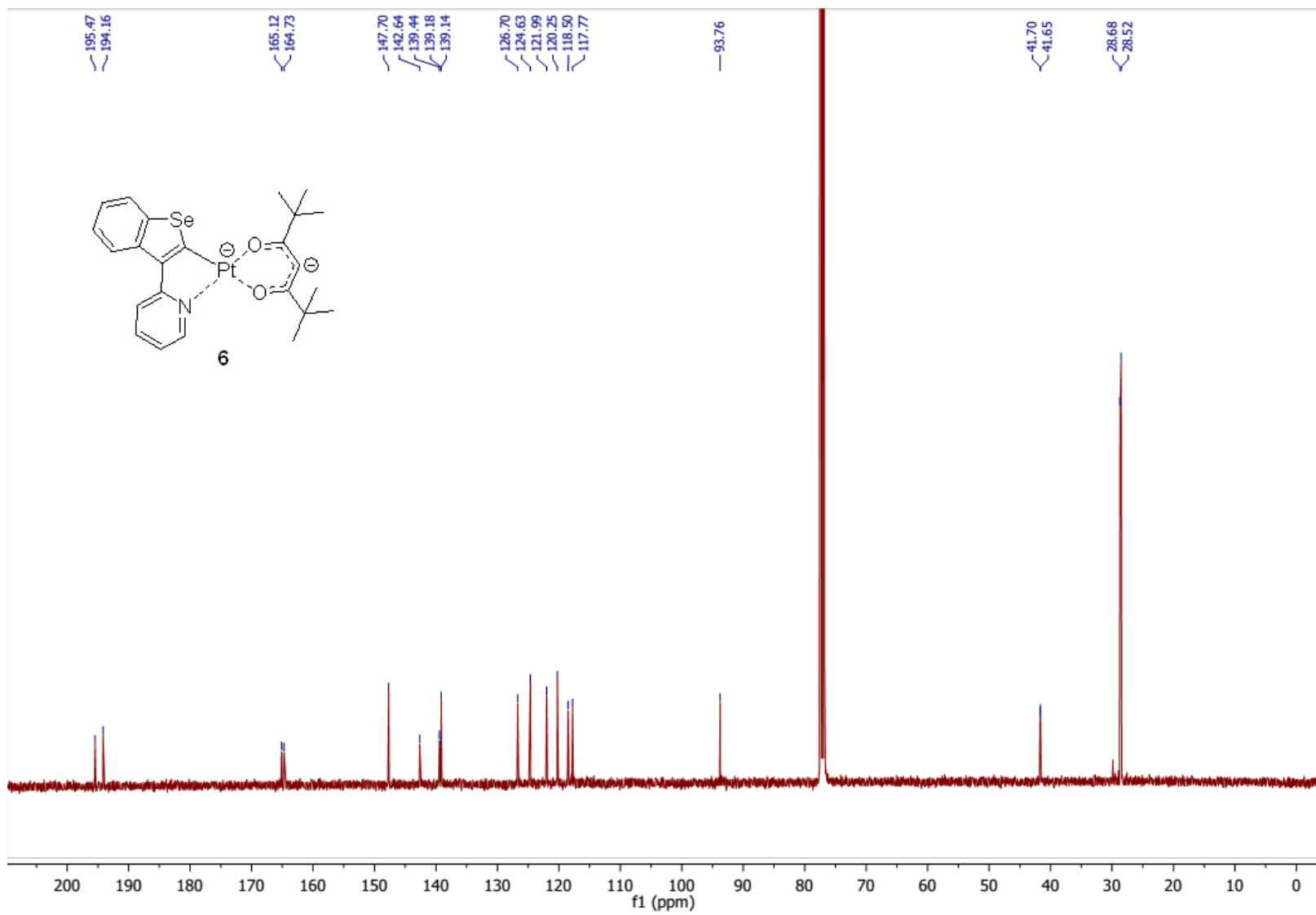




HRMS. Compound 3



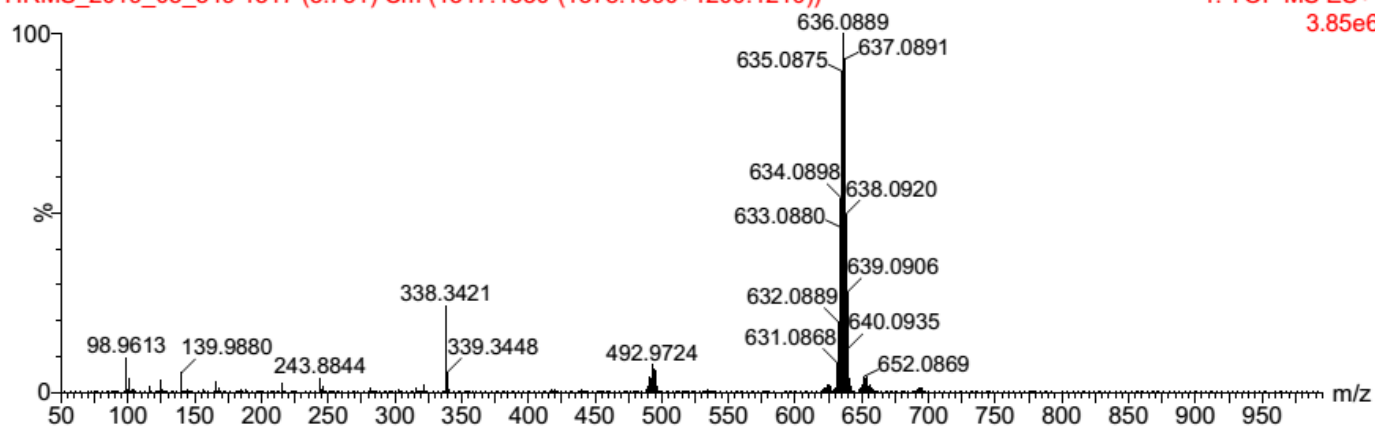




HRMS. Compound 6

HRMS_2019_05_349 1317 (3.751) Cm (1317:1330-(1378:1390+1200:1210))

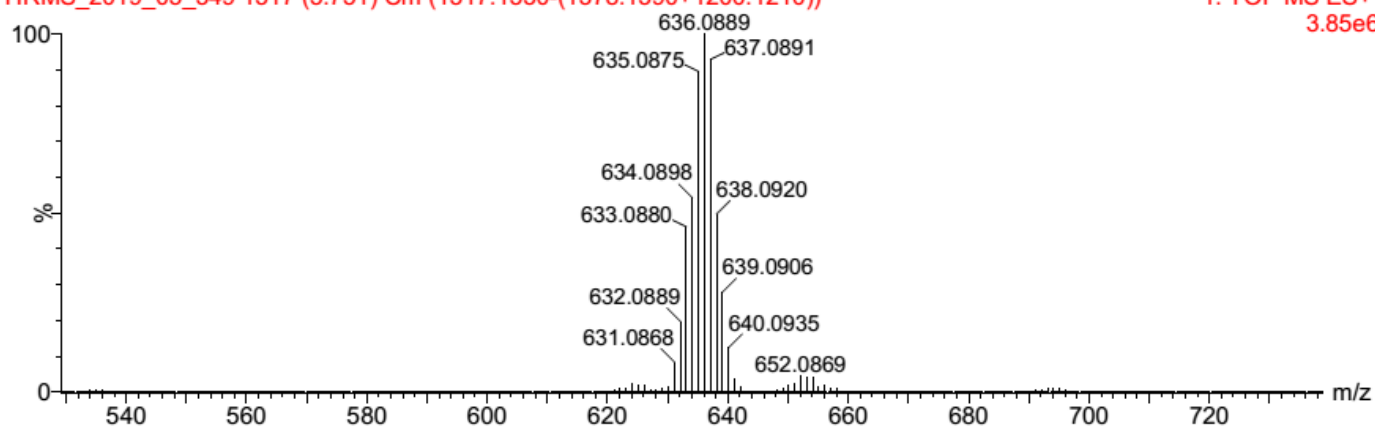
1: TOF MS ES+
3.85e6



761 Petrenko A-561

HRMS_2019_05_349 1317 (3.751) Cm (1317:1330-(1378:1390+1200:1210))

1: TOF MS ES+
3.85e6



Compound 3

Table 1 Crystal data and structure refinement for A508.

Identification code	A-508
Empirical formula	C ₂₄ H ₂₇ NO ₂ PtSe
Formula weight	635.52
Temperature/K	160.0(1)
Crystal system	Monoclinic
Space group	<i>P</i> 2 ₁ / <i>c</i>
<i>a</i> /Å	17.13173(12)
<i>b</i> /Å	5.77152(5)
<i>c</i> /Å	23.0206(2)
α /°	90
β /°	107.0499(8)
γ /°	90
Volume/Å ³	2176.15(3)
<i>Z</i>	4
ρ_{calc} /cm ³	1.9397
μ /mm ⁻¹	14.126
<i>F</i> (000)	1206.1
Crystal size/mm ³	0.01 × 0.02 × 0.10
Radiation	Cu K α (λ = 1.54184)
2 θ max. for data collection/°	155.0
Index ranges	-18 ≤ <i>h</i> ≤ 21, -7 ≤ <i>k</i> ≤ 7, -28 ≤ <i>l</i> ≤ 29
Reflections collected	25259
Independent reflections	4609 [<i>R</i> _{int} = 0.0396, <i>R</i> _{sigma} = 0.0203]

Data/restraints/parameters 4609/0/268

Goodness-of-fit on F^2 1.051

Final R indexes [$I \geq 2\sigma(I)$] $R_1 = 0.0354$, $wR_2 = 0.0779$

Final R indexes [all data] $R_1 = 0.0391$, $wR_2 = 0.0786$

Largest diff. peak/hole / $e \text{ \AA}^{-3}$ 3.19/-1.39

Table 2 Fractional Atomic Coordinates ($\times 10^4$) and Equivalent Isotropic Displacement Parameters ($\text{\AA}^2 \times 10^3$) for A508. U_{eq} is defined as 1/3 of the trace of the orthogonalised U_{ij} tensor.

Atom	x	y	z	$U(\text{eq})$
Pt1	2098.92(7)	3302.4(2)	2708.95(5)	17.25(7)
Se1	727.9(2)	-2800.7(7)	3244.91(17)	22.50(10)
O20	2790.1(13)	5100(4)	3427.9(10)	20.4(4)
O16	2572.2(13)	5145(4)	2118.0(10)	21.4(5)
N11	1443.0(16)	1307(5)	2025.5(13)	19.4(5)
C15	655(2)	-2184(7)	1761.7(17)	23.7(7)
C12	1335(2)	1732(6)	1432.8(16)	21.8(7)
C3	1596.2(18)	1180(6)	3179.8(15)	18.5(6)
C10	1096.5(17)	-606(6)	2193.8(15)	19.1(6)
C19	3347(2)	6546(5)	3402.7(17)	20.6(7)
C4	1877(2)	2674(7)	4269.7(16)	23.9(7)
C8	1142.1(19)	-900(6)	3928.7(15)	22.1(6)
C21	3486(2)	7523(6)	1774.2(15)	21.6(6)
C2	1196.1(18)	-624(6)	2834.1(15)	20.5(6)
C14	544(2)	-1744(6)	1152.1(19)	24.9(8)
C13	883(2)	255(7)	986.2(15)	26.1(7)

C22	3861(2)	7534(7)	4019.0(15)	23.1(7)
C17	3161(2)	6567(6)	2283.0(16)	20.1(7)
C7	1051(2)	-1259(7)	4502.4(17)	25.8(7)
C9	1560.4(18)	1065(7)	3797.8(15)	21.3(6)
C23	3519(2)	10184(6)	1797.1(18)	28.0(7)
C5	1783(2)	2307(8)	4836.8(16)	28.0(7)
C26	4731(2)	6581(7)	4149.6(19)	29.5(8)
C28	3881(2)	10192(7)	3991.9(17)	28.9(7)
C6	1374(2)	329(7)	4955.1(16)	29.2(8)
C27	3515(2)	6847(7)	4534.9(17)	29.1(8)
C24	4355(2)	6584(7)	1869(2)	31.1(9)
C18	3537(2)	7244(7)	2883.9(16)	27.0(7)
C25	2941(3)	6781(7)	1151.5(18)	30.8(8)

Table 3 Anisotropic Displacement Parameters ($\text{\AA}^2 \times 10^3$) for A508. The Anisotropic displacement factor exponent takes the form: $-2\pi^2[h^2a^*U_{11}+2hka^*b^*U_{12}+\dots]$.

Atom	U_{11}	U_{22}	U_{33}	U_{12}	U_{13}	U_{23}
Pt1	14.93(10)	17.76(11)	18.97(10)	-2.46(4)	4.83(6)	-0.40(4)
Se1	21.67(18)	19.01(18)	27.79(19)	-4.12(13)	8.76(14)	0.93(14)
O20	19.9(10)	18.9(12)	21.9(11)	-4.6(9)	5.5(8)	-2.4(9)
O16	20.6(10)	22.4(12)	20.8(10)	-6.2(9)	5.6(9)	1.7(9)
N11	15.5(12)	22.1(14)	20.5(13)	-1.5(10)	5.4(10)	-2.0(11)
C15	19.1(15)	21.9(16)	29.7(17)	-1.0(13)	6.5(13)	-5.9(14)
C12	16.9(15)	30(2)	17.8(16)	-1.7(12)	3.3(12)	-0.6(12)
C3	16.2(13)	15.6(14)	23.7(16)	1.4(12)	5.9(11)	2.1(13)
C10	12.3(12)	18.7(15)	25.0(15)	0.1(12)	3.4(11)	-0.3(12)

C19	17.2(15)	17.5(17)	26.1(17)	-1.1(11)	4.6(13)	-2.9(12)
C4	22.8(15)	23.4(17)	25.3(17)	-3.2(14)	6.5(13)	0.8(14)
C8	19.0(14)	21.7(17)	25.4(16)	0.6(13)	6.0(12)	3.2(13)
C21	21.9(15)	20.2(17)	23.8(16)	-0.6(14)	8.6(12)	1.2(14)
C2	15.1(13)	20.4(16)	26.6(16)	-2.5(12)	7.0(11)	0.6(13)
C14	21.0(16)	22.8(19)	29.1(19)	-1.8(12)	4.5(14)	-6.4(13)
C13	22.2(15)	35(2)	21.3(15)	-3.0(14)	6.2(12)	-4.6(14)
C22	19.1(15)	28.3(19)	20.8(15)	-3.2(14)	4.1(12)	-2.0(14)
C17	17.1(16)	21.8(18)	23.2(17)	-1.4(11)	8.7(12)	2.7(12)
C7	23.8(16)	26.3(17)	27.8(17)	-2.0(14)	8.0(13)	5.9(15)
C9	15.4(13)	24.6(17)	24.3(16)	-0.1(13)	6.5(12)	4.0(14)
C23	28.0(16)	21.1(17)	36.3(19)	-1.8(14)	11.4(14)	3.7(15)
C5	28.1(17)	33(2)	21.1(16)	-2.7(16)	4.0(13)	-2.7(15)
C26	21.3(17)	33(2)	30.7(19)	1.2(13)	1.9(15)	-2.9(14)
C28	29.8(17)	23.5(18)	31.2(18)	-3.1(14)	5.3(14)	-3.9(15)
C6	26.4(16)	41(2)	21.0(15)	2.6(15)	7.9(13)	6.8(15)
C27	29.1(18)	37(2)	20.7(17)	-6.9(14)	6.5(15)	-3.5(14)
C24	28.8(19)	31(2)	38(2)	3.1(14)	17.4(17)	3.6(15)
C18	25.4(16)	29.3(18)	25.8(17)	-11.7(15)	6.8(13)	-2.7(15)
C25	34(2)	33(2)	27.2(19)	-8.9(14)	11.6(16)	1.6(14)

Table 4 Bond Lengths for A508.

Atom	Atom	Length/Å	Atom	Atom	Length/Å
Pt1	O20	2.017(2)	C19	C18	1.387(5)
Pt1	O16	2.070(2)	C4	C9	1.411(5)

Pt1	N11	2.007(3)	C4	C5	1.378(5)
Pt1	C3	1.991(3)	C8	C7	1.390(5)
Se1	C8	1.879(4)	C8	C9	1.420(5)
Se1	C2	1.887(3)	C21	C17	1.540(5)
O20	C19	1.281(4)	C21	C23	1.537(5)
O16	C17	1.269(4)	C21	C24	1.538(5)
N11	C12	1.345(5)	C21	C25	1.525(5)
N11	C10	1.362(4)	C14	C13	1.394(5)
C15	C10	1.396(5)	C22	C26	1.535(5)
C15	C14	1.383(6)	C22	C28	1.536(5)
C12	C13	1.384(5)	C22	C27	1.527(5)
C3	C2	1.366(5)	C17	C18	1.400(5)
C3	C9	1.443(4)	C7	C6	1.376(6)
C10	C2	1.433(5)	C5	C6	1.408(6)
C19	C22	1.543(5)			

Table 5 Bond Angles for A508.

Atom	Atom	Atom	Angle/°	Atom	Atom	Atom	Angle/°
O16	Pt1	O20	91.50(9)	C23	C21	C17	110.5(3)
N11	Pt1	O20	175.94(10)	C24	C21	C17	108.5(3)
N11	Pt1	O16	90.97(10)	C24	C21	C23	108.8(3)
C3	Pt1	O20	96.51(11)	C25	C21	C17	110.9(3)
C3	Pt1	O16	171.50(12)	C25	C21	C23	108.6(3)
C3	Pt1	N11	80.88(13)	C25	C21	C24	109.5(3)

C2	Se1	C8	85.38(15)	C3	C2	Se1	115.5(2)
C19	O20	Pt1	124.3(2)	C10	C2	Se1	125.5(2)
C17	O16	Pt1	124.4(2)	C10	C2	C3	118.8(3)
C12	N11	Pt1	124.7(2)	C13	C14	C15	119.0(3)
C10	N11	Pt1	115.6(2)	C14	C13	C12	119.6(3)
C10	N11	C12	119.6(3)	C26	C22	C19	107.9(3)
C14	C15	C10	119.2(3)	C28	C22	C19	110.2(3)
C13	C12	N11	121.5(3)	C28	C22	C26	109.5(3)
C2	C3	Pt1	112.0(2)	C27	C22	C19	111.9(3)
C9	C3	Pt1	135.7(3)	C27	C22	C26	109.3(3)
C9	C3	C2	112.3(3)	C27	C22	C28	108.0(3)
C15	C10	N11	121.1(3)	C21	C17	O16	115.9(3)
C2	C10	N11	111.6(3)	C18	C17	O16	124.8(3)
C2	C10	C15	127.2(3)	C18	C17	C21	119.2(3)
C22	C19	O20	115.5(3)	C6	C7	C8	119.2(3)
C18	C19	O20	126.5(3)	C4	C9	C3	127.6(3)
C18	C19	C22	118.0(3)	C8	C9	C3	114.6(3)
C5	C4	C9	120.2(3)	C8	C9	C4	117.8(3)
C7	C8	Se1	126.1(3)	C6	C5	C4	120.8(4)
C9	C8	Se1	112.2(2)	C5	C6	C7	120.4(3)
C9	C8	C7	121.7(3)	C17	C18	C19	127.9(3)

Table 6 Hydrogen Atom Coordinates ($\text{\AA}\times 10^4$) and Isotropic Displacement Parameters ($\text{\AA}^2\times 10^3$) for A508.

Atom	x	y	z	$U(\text{eq})$
------	---	---	---	----------------

H15	438(2)	-3514(7)	1882.2(17)	28.5(8)
H12	1569(2)	3047(6)	1320.3(16)	26.2(9)
H4	2150(2)	3986(7)	4197.8(16)	28.7(8)
H14	248(2)	-2767(6)	857.2(19)	29.9(9)
H13	805(2)	594(7)	578.3(15)	31.3(8)
H7	775(2)	-2557(7)	4579.4(17)	31.0(8)
H23a	2992(5)	10782(7)	1785(14)	42.0(11)
H23b	3914(13)	10673(6)	2166(6)	42.0(11)
H23c	3673(18)	10759(7)	1455(7)	42.0(11)
H5	1992(2)	3379(8)	5144.9(16)	33.6(9)
H26a	4715(3)	4919(7)	4135(15)	44.3(12)
H26b	4972(7)	7150(50)	3850(9)	44.3(12)
H26c	5053(6)	7080(50)	4546(6)	44.3(12)
H28a	4136(17)	10665(7)	3691(10)	43.4(11)
H28b	3334(2)	10784(7)	3886(13)	43.4(11)
H28c	4187(16)	10790(7)	4381(4)	43.4(11)
H6	1321(2)	94(7)	5341.5(16)	35.1(9)
H27a	2970(8)	7440(50)	4454(8)	43.6(12)
H27b	3505(19)	5189(7)	4565(10)	43.6(12)
H27c	3853(12)	7480(50)	4910(3)	43.6(12)
H24a	4704(5)	7110(50)	2253(7)	46.6(13)
H24b	4343(4)	4922(7)	1864(15)	46.6(13)
H24c	4561(8)	7130(50)	1548(9)	46.6(13)
H18	3966(2)	8289(7)	2942.4(16)	32.3(9)
H25a	2912(17)	5121(7)	1132(6)	46.3(13)

H25b	2403 (6)	7410 (50)	1088 (7)	46.3 (13)
H25c	3165 (12)	7350 (50)	842 (2)	46.3 (13)

Compound 6

Table 1 Crystal data and structure refinement for A561new.

Identification code	A-561
Empirical formula	C ₂₆ H ₃₀ N ₂ O ₂ PtSe
Formula weight	676.57
Temperature/K	150.0(1)
Crystal system	orthorhombic
Space group	<i>Pnma</i>
<i>a</i> /Å	35.3302(2)
<i>b</i> /Å	6.8420(1)
<i>c</i> /Å	10.3388(1)
α /°	90
β /°	90
γ /°	90
Volume/Å ³	2499.15(3)
<i>Z</i>	4
ρ_{calc} /cm ³	1.798
μ /mm ⁻¹	12.358
<i>F</i> (000)	1312.0
Crystal size/mm ³	0.08 × 0.04 × 0.03
Radiation	CuK α (λ = 1.54184)
2 Θ max. for data collection/°	155.0
Index ranges	-43 ≤ <i>h</i> ≤ 44, -8 ≤ <i>k</i> ≤ 8, -11 ≤ <i>l</i> ≤ 13
Reflections collected	25004
Independent reflections	2865 [<i>R</i> _{int} = 0.0648, <i>R</i> _{sigma} = 0.0291]
Data/restraints/parameters	2865/0/187
Goodness-of-fit on <i>F</i> ²	1.222
Final <i>R</i> indexes [<i>I</i> ≥ 2 σ (<i>I</i>)]	<i>R</i> ₁ = 0.0339, <i>wR</i> ₂ = 0.0927
Final <i>R</i> indexes [all data]	<i>R</i> ₁ = 0.0339, <i>wR</i> ₂ = 0.0927
Largest diff. peak/hole / e Å ⁻³	2.14/-2.14

Table 2 Fractional Atomic Coordinates ($\times 10^4$) and Equivalent Isotropic Displacement Parameters ($\text{\AA}^2 \times 10^3$) for A561new. U_{eq} is defined as 1/3 of the trace of the orthogonalised U_{ij} tensor.

Atom	<i>x</i>	<i>y</i>	<i>z</i>	<i>U</i> (eq)
Pt1	5884.1(2)	7500	5932.3(2)	14.62(11)
Se1	5242.5(2)	7500	8443.7(5)	24.58(16)
C2	5386.5(15)	7500	6700(5)	18.4(10)
C3	5077.0(17)	7500	5891(5)	17.2(11)
C4	4342.2(17)	7500	5983(5)	23.3(12)
C5	4025.6(17)	7500	6772(7)	26.1(12)
C6	4060.0(17)	7500	8108(7)	26.8(13)
C7	4417.6(17)	7500	8688(6)	26.0(11)
C8	4732.0(16)	7500	7885(6)	22.3(11)
C9	4706.0(15)	7500	6521(5)	18.8(10)
C10	5184.0(14)	7500	4529(5)	13.9(9)
N11	5566.8(13)	7500	4345(4)	15.5(8)
C12	5711.1(15)	7500	3130(5)	19.8(10)
C13	5489.0(17)	7500	2052(5)	23.3(11)
C14	5100.5(17)	7500	2215(6)	26.0(12)
C15	4946.4(16)	7500	3431(5)	22.2(11)
C1'	7040.1(15)	7500	4468(6)	20.7(10)
C2'	6716.2(15)	7500	5449(5)	17.8(10)
C3'	6781.7(15)	7500	6775(5)	19.0(10)
C4'	6515.4(16)	7500	7773(5)	18.6(10)
C5'	6639.5(17)	7500	9189(5)	19.7(11)
O2'	6389.0(10)	7500	4923(4)	21.9(8)
O4'	6152.3(10)	7500	7620(3)	19.2(7)
C6'	7433.8(16)	7500	5095(6)	27.2(12)
C7'	6998.4(12)	5664(7)	3620(4)	29.6(9)
C8'	7066.1(18)	7500	9392(7)	33.6(14)
C9'	6468.9(14)	5681(8)	9840(4)	39.2(11)
C1S	6403(2)	2500	6593(8)	42.5(17)
C2S	6804(2)	2500	6760(7)	33.5(14)
N1S	7127.7(19)	2500	6876(7)	45.8(15)

Table 3 Anisotropic Displacement Parameters ($\text{\AA}^2 \times 10^3$) for A561new. The Anisotropic displacement factor exponent takes the form:

$$-2\pi^2[h^2a^*U_{11}+2hka^*b^*U_{12}+\dots].$$

Atom	U_{11}	U_{22}	U_{33}	U_{23}	U_{13}	U_{12}
Pt1	11.27(15)	17.26(15)	15.33(16)	0	-0.04(6)	0
Se1	18.3(3)	39.6(4)	15.8(3)	0	0.8(2)	0
C2	17(2)	19(2)	19(2)	0	5.9(19)	0
C3	15(3)	19(3)	18(3)	0	2.5(18)	0
C4	15(3)	26(3)	28(3)	0	0.8(19)	0
C5	16(2)	25(3)	37(3)	0	2(2)	0
C6	18(2)	27(3)	36(3)	0	11(2)	0
C7	23(3)	29(3)	27(3)	0	4(2)	0
C8	20(3)	22(3)	24(3)	0	2(2)	0
C9	16(2)	15(2)	25(3)	0	0.7(19)	0
C10	12(2)	11(2)	18(2)	0	0.6(18)	0
N11	15(2)	15(2)	16.5(18)	0	1.7(17)	0
C12	17(2)	23(3)	19(2)	0	1(2)	0
C13	30(3)	25(3)	15(2)	0	0(2)	0
C14	26(3)	29(3)	23(3)	0	-13(2)	0
C15	15(2)	27(3)	24(3)	0	-4(2)	0
C1'	16(2)	24(3)	22(3)	0	4(2)	0
C2'	16(2)	15(2)	22(3)	0	-1(2)	0
C3'	15(2)	21(2)	20(3)	0	0.6(19)	0
C4'	20(2)	16(2)	20(2)	0	3(2)	0
C5'	18(3)	23(3)	18(3)	0	-0.1(18)	0
O2'	13.8(17)	35(2)	16.9(17)	0	1.5(14)	0
O4'	14.9(16)	28.2(19)	14.6(16)	0	2.3(13)	0
C6'	16(2)	36(3)	29(3)	0	4(2)	0
C7'	26.1(19)	36(2)	26.4(19)	-7.6(18)	7.2(15)	0.1(18)
C8'	24(3)	52(4)	25(3)	0	-5(2)	0
C9'	44(3)	49(3)	24.2(19)	13(2)	-8.2(18)	-16(2)
C1S	41(4)	35(3)	52(4)	0	-17(3)	0
C2S	46(4)	26(3)	29(3)	0	-9(3)	0
N1S	42(3)	41(3)	55(4)	0	-14(3)	0

Table 4 Bond Lengths for A561new.

Atom	Atom	Length/Å	Atom	Atom	Length/Å
Pt1	C2	1.929(5)	C12	C13	1.363(8)
Pt1	N11	1.987(5)	C13	C14	1.383(9)
Pt1	O2'	2.067(4)	C14	C15	1.370(9)
Pt1	O4'	1.985(4)	C1'	C2'	1.529(7)
Se1	C2	1.874(5)	C1'	C6'	1.535(8)
Se1	C8	1.894(6)	C1'	C7'	1.539(5)
C2	C3	1.376(8)	C1'	C7' ¹	1.539(5)
C3	C9	1.463(7)	C2'	C3'	1.390(8)
C3	C10	1.458(7)	C2'	O2'	1.278(7)
C4	C5	1.384(8)	C3'	C4'	1.396(7)
C4	C9	1.400(8)	C4'	C5'	1.528(7)
C5	C6	1.387(10)	C4'	O4'	1.292(7)
C6	C7	1.399(9)	C5'	C8'	1.522(8)
C7	C8	1.387(8)	C5'	C9' ¹	1.538(6)
C8	C9	1.413(8)	C5'	C9'	1.538(6)
C10	N11	1.366(6)	C1S	C2S	1.429(11)
C10	C15	1.412(7)	C2S	N1S	1.148(10)
N11	C12	1.356(7)			

 $^1+X,3/2-Y,+Z$

Table 5 Bond Angles for A561new.

Atom	Atom	Atom	Angle/°	Atom	Atom	Atom	Angle/°
C2	Pt1	N11	79.9(2)	C12	N11	C10	120.1(5)
C2	Pt1	O2'	173.95(19)	N11	C12	C13	122.8(5)
C2	Pt1	O4'	94.22(19)	C12	C13	C14	118.1(5)
N11	Pt1	O2'	94.01(16)	C15	C14	C13	120.4(5)
O4'	Pt1	N11	174.16(16)	C14	C15	C10	120.1(5)
O4'	Pt1	O2'	91.83(15)	C2'	C1'	C6'	113.4(5)
C2	Se1	C8	88.0(2)	C2'	C1'	C7' ¹	107.8(3)
Se1	C2	Pt1	130.0(3)	C2'	C1'	C7'	107.8(3)
C3	C2	Pt1	118.3(4)	C6'	C1'	C7' ¹	109.1(3)
C3	C2	Se1	111.6(4)	C6'	C1'	C7'	109.1(3)
C2	C3	C9	116.2(5)	C7'	C1'	C7' ¹	109.4(5)
C2	C3	C10	112.4(5)	C3'	C2'	C1'	122.0(5)
C10	C3	C9	131.4(5)	O2'	C2'	C1'	113.2(5)
C5	C4	C9	120.5(5)	O2'	C2'	C3'	124.8(5)
C4	C5	C6	121.1(6)	C2'	C3'	C4'	128.0(5)

C5	C6	C7	120.4(5)	C3'	C4'	C5'	121.0(5)
C8	C7	C6	117.8(6)	O4'	C4'	C3'	125.4(5)
C7	C8	Se1	125.4(5)	O4'	C4'	C5'	113.7(5)
C7	C8	C9	123.1(5)	C4'	C5'	C9'	107.9(3)
C9	C8	Se1	111.5(4)	C4'	C5'	C9 ¹	107.9(3)
C4	C9	C3	130.2(5)	C8'	C5'	C4'	114.6(5)
C4	C9	C8	117.1(5)	C8'	C5'	C9 ¹	109.1(3)
C8	C9	C3	112.7(5)	C8'	C5'	C9'	109.1(3)
N11	C10	C3	113.0(5)	C9'	C5'	C9 ¹	108.0(5)
N11	C10	C15	118.5(5)	C2'	O2'	Pt1	124.5(3)
C15	C10	C3	128.5(5)	C4'	O4'	Pt1	125.5(3)
C10	N11	Pt1	116.3(4)	N1S	C2S	C1S	179.0(8)
C12	N11	Pt1	123.6(4)				

¹+X,3/2-Y,+Z

Table 6 Hydrogen Atom Coordinates ($\text{\AA}\times 10^4$) and Isotropic Displacement Parameters ($\text{\AA}^2\times 10^3$) for A561new.

Atom	X	y	z	U(eq)
H4	4313.12	7500	5088.93	28
H5	3785.96	7500	6399.45	31
H6	3843.88	7500	8621.68	32
H7	4443.8	7500	9583.51	31
H12	5972.61	7500	3027.04	24
H13	5595.69	7500	1229.55	28
H14	4942.84	7500	1494.92	31
H15	4684.84	7500	3533.91	27
H3'	7034.23	7500	7028.57	23
H6'A	7624.12	7500	4432.7	41
H6'B	7461.62	8645.6	5622.7	41
H7'A	7198.96	5630.35	2993.67	44
H7'B	7011.26	4519.31	4154.34	44
H7'C	6758.86	5698.73	3181.67	44
H8'A	7121.29	7500	10301.18	50
H8'B	7173.09	8645.6	9000.07	50
H9'A	6199.72	5674.33	9714.43	59
H9'B	6576.56	4525.97	9462.82	59
H9'C	6524.05	5708.86	10748.97	59
H1SA	6280.79	2500	7391.39	64
H1SB	6335.19	1354.4	6091.39	64

Computational details

The structures of the **3** and **6** complexes in the ground electronic state were optimized at the DFT level in a gas phase using the B3LYP¹ hybrid functional and combined basis set – Lanl2DZ² for the Pt atoms and 6-31G(d)³ basis set for the rest of atoms (C, N, O, Se and H). The structure of both complexes in the first excited triplet state was optimized by the same method using spin-unrestricted SCF formalism. The vertical electronic singlet-singlet and singlet-triplet electronic transitions were then calculated by the time-dependent (TD) DFT method⁴ using the same B3LYP/Lanl2DZ(Pt)/6-31G(d)(C,N,O,Se,H) approximation. In order to take into account the solvent effects vertical spectra were computed using the polarizable continuum model (PCM)⁵, taking the toluene ($\epsilon = 2.37$) as a model solvent. All these calculations were performed using the Gaussian16 software [<https://gaussian.com/citation/>].

Based on the T₁ state optimized geometries from the previous step the spin-orbit coupling (SOC) effects were treated as a perturbation based on the scalar relativistic (SR) orbitals after SCF and TDDFT calculations (pSOC-TDDFT)⁶; B3LYP functional and Slater-type TZP all-electron basis set⁷ were used for this sort of calculations. The SOC calculations for both studied systems were carried out using the ADF2018 package [https://www.scm.com/doc/ADF/Required_citations.html].

The SOC matrix elements, $\langle S_i | \hat{H}_{SO} | T_j \rangle$ were calculated as root mean squares, i.e. as square root of the sum of squares of spin-orbit coupling matrix elements of all triplet state sublevels ($m=0,\pm 1$) of the uncoupled states⁸ [[10.1021/jacs.6b12124](https://doi.org/10.1021/jacs.6b12124)]:

$$\langle S_i | \hat{H}_{SO} | T_j \rangle = \sqrt{\sum_{m=0,\pm 1} \langle S_i | \hat{H}_{SO} | T_j^m \rangle^2}. \quad (1)$$

The spin-orbit coupling operator \hat{H}_{SO} was considered in our calculations within the zeroth-order regular approximation (ZORA) in accordance with the following expression:

$$\hat{H}_{SO} = \frac{c^2}{(2c^2 - V)^2} \boldsymbol{\sigma}(\nabla V \cdot \mathbf{p}), \quad (2)$$

where $\boldsymbol{\sigma}$ – Pauli spin matrix vector, \mathbf{p} – the linear momentum operator; c – speed of light, V – Kohn–Sham potential. The radiative lifetimes (τ) for the singlet and triplet states of interest were estimated according to^{9,10}:

$$\tau = \frac{c^3}{2(\Delta E^2)f}, \quad (3)$$

where ΔE and f – the energy and intensity of the corresponding singlet-singlet or singlet-triplet transitions with accounting of SOC perturbations. For the triplet states the partial radiative lifetimes for each separate spin sublevel (τ^m , $m=0,\pm 1$) were calculated.

Accounting for the quite large zero-field splitting (ZFS) of T_1^m sublevels for both LLT-30 and LLT-31 complexes due to the presence of heavy Pt and Se atoms the Boltzmann-weighted averaging procedure was used for the estimation of average phosphorescence lifetime (τ_{av})^{9,10}:

$$\tau_{av} = \frac{1 + e^{[-\Delta E_{m=0}^{m=-1}/k_b T]} + e^{[-\Delta E_{m=1}^{m=-1}/k_b T]}}{k_{m=-1} + k_{m=0} e^{[-\Delta E_{m=0}^{m=-1}/k_b T]} + k_{m=1} e^{[-\Delta E_{m=1}^{m=-1}/k_b T]}}, \quad (4)$$

where $\Delta E_{m=0}^{m=-1}$ and $\Delta E_{m=1}^{m=-1}$ correspond to the energy difference between the triplet state spin-sublevels with $m = -1, 0$ and with $m = -1, 1$ respectively, $k_{m=-1}$, $k_{m=0}$ and $k_{m=1}$ – decay rates for the individual spin-sublevels of the T_1 state ($k_m = 1/\tau^m$), k_b – Boltzmann constant, T – temperature (298 K which is the same as in experiment).

Materials

Molybdenum trioxide (MoO_3), N,N'-di(1-naphthyl)-N,N'-diphenyl-(1,1'-biphenyl)-4,4'-diamine (NPB), 1,3-bis(9-carbazolyl)benzene (mCP), diphenyl-4-triphenylsilyl-phenylphosphineoxide (TSPO1) and 2,2',2''-(1,3,5-benzinetriyl)-tris(1-phenyl-1-*H*-benzimidazole) (TPBi) were obtained from either Sigma Aldrich or Lumtec.

Instrumentation

Cyclic voltammetry (CV) measurements were performed using a micro-Autolab III (Metrohm Autolab) potentiostat equipped with a standard three-electrode configuration. A three-electrode cell equipped with a glassy carbon-working electrode, an Ag/AgNO₃ (0.01 M in anhydrous acetonitrile) reference electrode and a Pt wire counter electrode were employed. The measurements were performed under argon atmosphere at 50 mV/s potential rate at room temperature. Oxidation potentials ($E_{1/2}$ vs Fc) for quasi reversible oxidation were collected as average values of the anodic and cathodic peak potentials, E_{pa} and E_{pc} , respectively. Ionization potentials (I_p^{CV}) were estimated from the onset oxidation potential using the relationship $I_p^{CV} =$

4.8 + E_{ox} vs Fc. Electron affinity (E_A) values were obtained from the reduction potentials using the approximation $E_A = 4.8 + E_{red}$ vs Fc.

Electron photoemission spectrometry was used to determine the ionization potentials (IP) of the layers of the synthesized compounds. For the recording of the photoelectron emission spectra, the layers were prepared by drop-casting chloroform solutions of the materials on cleaned indium tin oxide (ITO)-coated glass substrates. The negative voltage of 300 V was applied to the sample substrate. The deep UV deuterium light source ASBN-D130-CM and CM110 1/8 m monochromator were used for the illumination of the samples with the monochromatic light. A 6517B Keithley electrometer was connected to the counter-electrode for the measurement of the photocurrent which was flowing in the circuit under illumination. Energy scan of the incident photons was performed while increasing the photon energy. The photocurrent (which is attributed to dU/dt) is dependent on the incident light photon energy ($h\nu$). The I_p was estimated as the intersection points of the extrapolated linear part of the dependence $(dU/dt)^{1/2} = f(h\nu)$ and the $h\nu$ axis (i.e. the $h\nu$ value at zero photocurrent) [1].

Emission and UV/Vis absorbance spectra of the compounds in solutions (10^{-5} M) and solid films were recorded using the Edinburgh Instruments FLS980 and Avantes spectrometers, respectively. The excitation wavelength of 350 nm were selected for recording PL spectra. Photoluminescence decay curves were taken exploiting the PicoQuant LDH-D-C-375 laser (wavelength 374 nm) as the excitation source. Photoluminescence quantum yields (PLQY) were measured using an integrated sphere (inner diameter of 120 mm) on Edinburgh Instruments FLS980 spectrometer. Electroluminescent devices were fabricated by spin-coating of light-emitting layers and by vacuum deposition of additional organic and metal layers onto pre-cleaned ITO coated glass substrates under vacuum higher than 2×10^{-6} mBar. ITO-coated glass substrates with a sheet resistance of 15 Ω /sq were pre-patterned getting seven independent devices with area 6 mm². Density-voltage and luminance-voltage characteristics were recorded utilizing certificated photodiode PH100-Si-HA-D0 together with the PC-Based Power and Energy Monitor 11S-LINK (from STANDA) and Keithley 2400C source meter. Electroluminescence (EL) spectra were taken by the Avantes AvaSpec-2048XL spectrometer. Device efficiencies were calculated using the luminance, current density, and EL spectra.

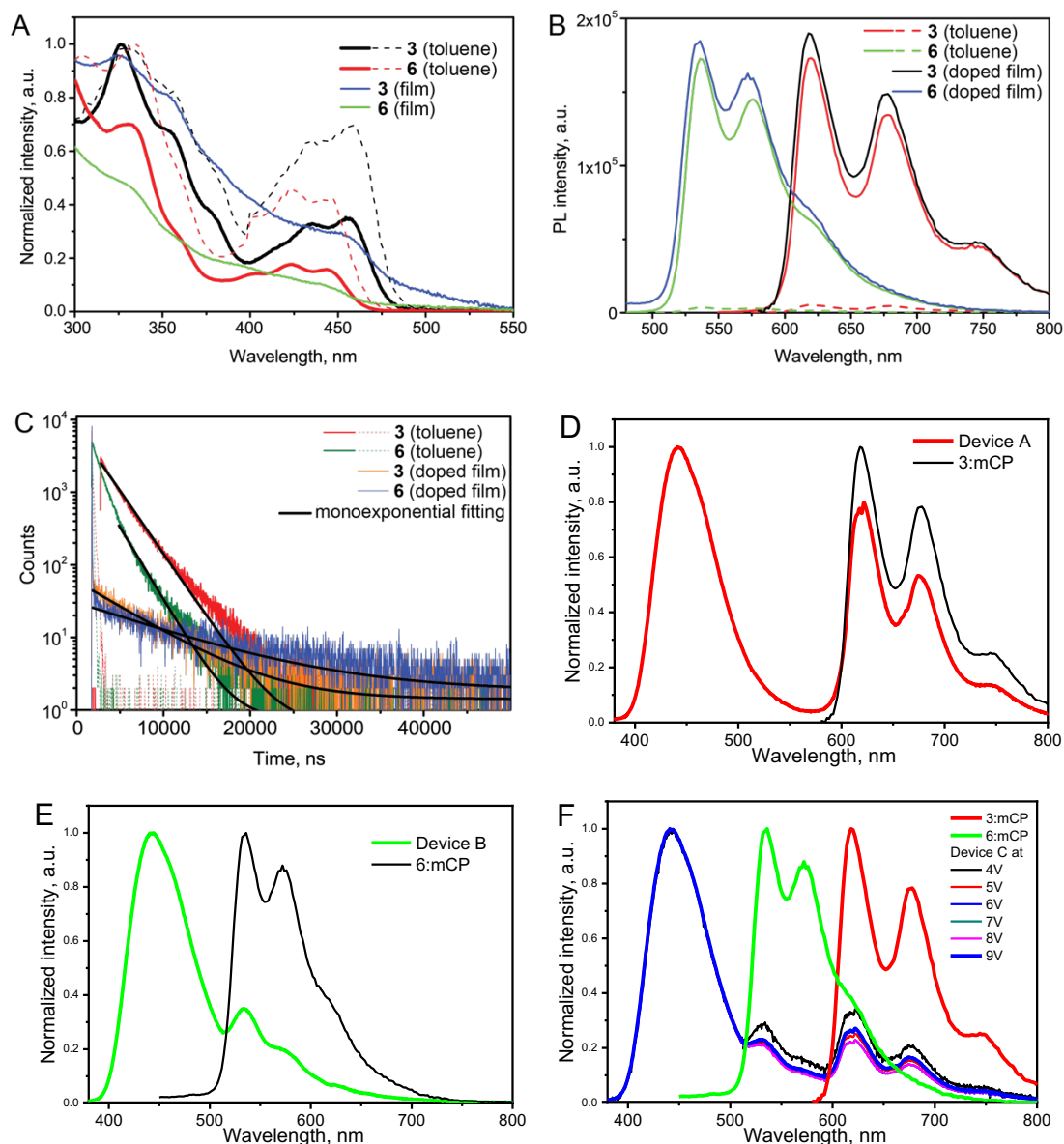


Figure S1. Absorption (solid lines) and excitation spectra (dashed lines) (a); phosphorescence spectra (b); and phosphorescence decays (c) of deoxygenated (solid lines) and non-deoxygenated (dashed lines) toluene solutions and solid films of complexes **3** and **6**. Doped films were spin-coated using mCP as the host with a 0.5wt.% of the dopant. EL spectra of devices A (d), B (e), C (f) and PL spectra of corresponding doped films of 3:mCP and/or 6:mCP.

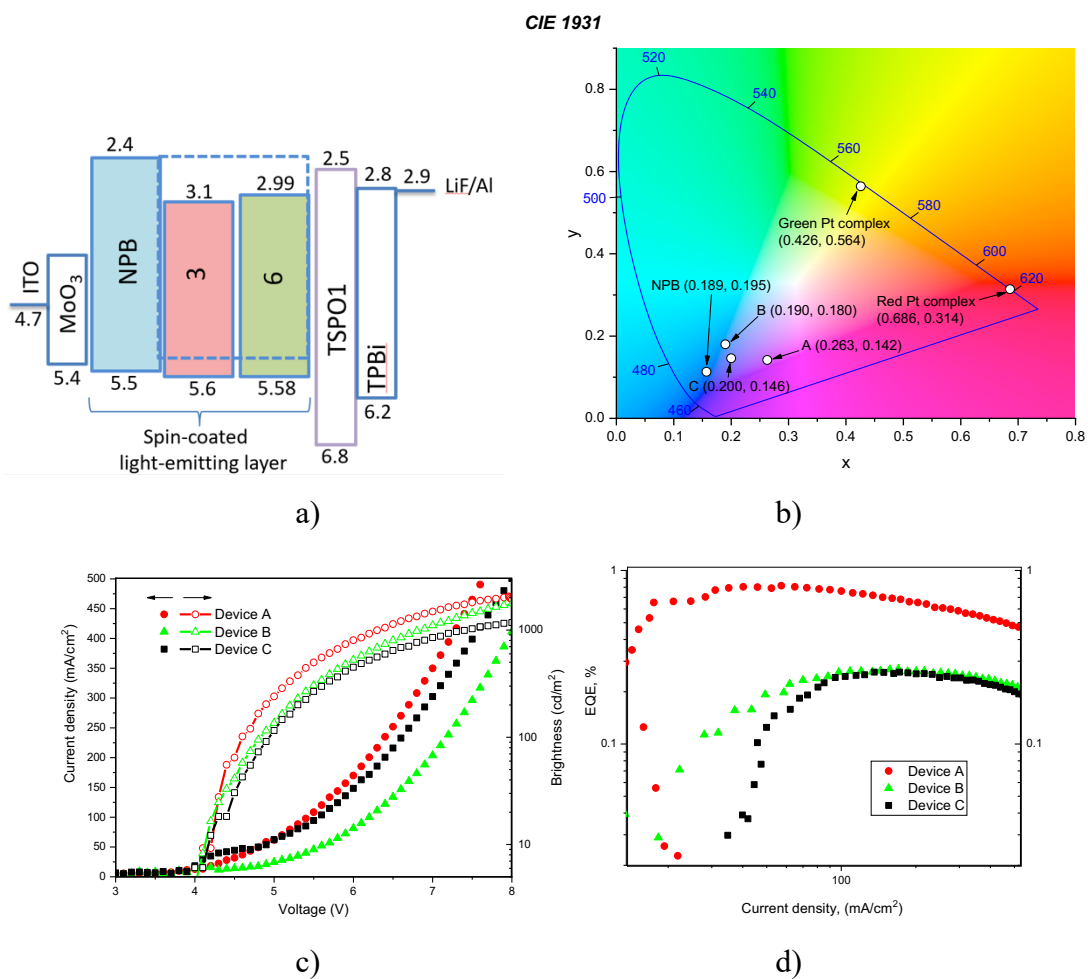


Figure S2. Equilibrium energy diagram (a); CIE 1931 coordinates for emission of designed emitters **3**, **6** and fabricated devices A-D (b); current density and brightness versus voltage (c); and external quantum efficiency versus current density (cd) characteristics.

Table SX. Cartesian coordinates for the **3** complex in the ground electronic state optimized by the B3LYP/Lan12DZ(Pt)/6-31G(d)(C,N,O,Se,H) method.

8	-1.092127000	1.509884000	0.000243000
6	-2.358029000	1.733130000	0.000320000
6	-3.381321000	0.773743000	-0.000042000
6	-3.253512000	-0.626252000	-0.000207000
8	-2.145905000	-1.255693000	0.000089000
6	-4.534019000	-1.496428000	-0.000771000
6	-2.776934000	3.226901000	0.000769000
6	-3.616108000	3.523691000	-1.265196000
6	-3.615796000	3.522963000	1.267133000
6	-1.552041000	4.155840000	0.000890000
6	-5.367077000	-1.185130000	-1.266205000
6	-4.170512000	-2.991699000	-0.000899000
6	-5.367945000	-1.185564000	1.264198000
1	-4.391294000	1.160042000	-0.000173000
1	-3.890390000	4.585358000	-1.286736000
1	-3.045981000	3.304063000	-2.175017000
1	-4.540674000	2.939338000	-1.298017000
1	-3.890132000	4.584602000	1.289325000
1	-4.540304000	2.938524000	1.299888000
1	-3.045399000	3.302876000	2.176674000
1	-1.888981000	5.199068000	0.001186000
1	-0.929808000	4.000769000	0.886954000
1	-0.930016000	4.001240000	-0.885410000
1	-6.261604000	-1.819410000	-1.288614000
1	-5.696467000	-0.141900000	-1.297187000
1	-4.789883000	-1.382876000	-2.176680000
1	-5.087458000	-3.592419000	-0.001359000
1	-3.586484000	-3.261268000	-0.886440000
1	-3.587161000	-3.261581000	0.884991000
1	-6.262488000	-1.819850000	1.285775000
1	-4.791378000	-1.383625000	2.175003000
1	-5.697363000	-0.142347000	1.295317000
78	-0.219102000	-0.358458000	0.000079000
6	1.710678000	0.208345000	-0.000046000
7	0.661870000	-2.193798000	0.000190000
6	2.403824000	1.478583000	-0.000355000
6	3.822993000	1.386598000	-0.000338000
34	4.420188000	-0.408981000	0.000022000
6	2.577142000	-0.865890000	0.000109000
6	2.032989000	-2.190438000	0.000287000
6	2.731153000	-3.407943000	0.000552000
6	2.028675000	-4.604800000	0.000677000
6	0.629515000	-4.582579000	0.000534000
6	-0.017200000	-3.353644000	0.000293000
6	4.634464000	2.522276000	-0.000612000
6	4.031357000	3.777063000	-0.000922000
6	2.631424000	3.894495000	-0.000972000
6	1.827193000	2.762889000	-0.000697000
1	3.816084000	-3.396667000	0.000660000
1	2.564065000	-5.549988000	0.000891000
1	0.046106000	-5.496557000	0.000605000
1	-1.096055000	-3.256323000	0.000180000
1	5.716931000	2.432200000	-0.000596000
1	4.651715000	4.669460000	-0.001137000
1	2.174369000	4.880486000	-0.001231000
1	0.749286000	2.838055000	-0.000741000

Table SX. Cartesian coordinates for the **6** complex in the ground electronic state optimized by the B3LYP/Lan12DZ(Pt)/6-31G(d)(C,N,O,Se,H) method.

78	0.293129000	0.387971000	-0.000107000
6	-1.547077000	-0.266690000	-0.000034000
7	-0.729679000	2.142665000	-0.000014000
34	-2.174969000	-2.029491000	-0.000057000
6	-3.933956000	-1.313354000	0.000063000
6	-2.578194000	0.663580000	0.000027000
6	-2.104946000	2.037354000	0.000014000
6	-2.857247000	3.224598000	-0.000006000
6	-2.225290000	4.461351000	-0.000013000
6	-0.829850000	4.530003000	0.000001000
6	-0.118604000	3.338831000	0.000002000
1	-3.936267000	3.176739000	-0.000027000
1	-2.821238000	5.369778000	-0.000041000
1	-0.301867000	5.476975000	0.000011000
1	0.965015000	3.302263000	-0.000010000
6	-3.927556000	0.107957000	0.000085000
6	-5.114918000	-2.054293000	0.000113000
6	-6.336591000	-1.386362000	0.000180000
6	-6.361670000	0.014016000	0.000192000
6	-5.181449000	0.751195000	0.000146000
1	-5.253645000	1.831831000	0.000152000
1	-7.314124000	0.537298000	0.000243000
1	-7.264752000	-1.950892000	0.000224000
1	-5.082180000	-3.140226000	0.000100000
8	1.143434000	-1.460089000	-0.000301000
6	2.404028000	-1.702911000	-0.000031000
6	3.433687000	-0.749718000	0.000148000
6	3.312446000	0.653756000	0.000014000
8	2.210820000	1.297916000	-0.000126000
6	4.599478000	1.514261000	0.000115000
6	2.769135000	-3.206479000	0.000032000
6	3.597239000	-3.533286000	-1.264889000
6	3.596098000	-3.533340000	1.265694000
6	1.497050000	-4.073783000	-0.000566000
6	5.431100000	1.197509000	-1.264951000
6	4.245524000	3.012014000	0.000086000
6	5.430861000	1.197496000	1.265332000
1	4.441788000	-1.142227000	0.000350000
1	3.834479000	-4.603799000	-1.285911000
1	3.036003000	-3.294185000	-2.175274000
1	4.541729000	-2.980878000	-1.295923000
1	3.833426000	-4.603832000	1.286831000
1	4.540494000	-2.980822000	1.297650000
1	3.033987000	-3.294380000	2.175575000
1	1.779690000	-5.133059000	-0.000505000
1	0.880094000	-3.882652000	0.882180000
1	0.880860000	-3.882554000	-0.883830000
1	6.329755000	1.825933000	-1.286631000
1	5.753628000	0.152135000	-1.296200000
1	4.855768000	1.399541000	-2.175669000
1	5.166594000	3.606463000	0.000098000
1	3.662684000	3.285218000	-0.884953000
1	3.662661000	3.285242000	0.885105000
1	6.329570000	1.825838000	1.287136000
1	4.855396000	1.399615000	2.175946000
1	5.753289000	0.152091000	1.296677000

Table SX. Cartesian coordinates for the **3** complex in the T₁ excited state optimized by the UB3LYP/Lanl2DZ(Pt)/6-31G(d)(C,N,O,Se,H) method.

8	-1.105068000	1.516894000	0.000373000
6	-2.372049000	1.722867000	0.000639000
6	-3.383932000	0.749937000	-0.000166000
6	-3.240141000	-0.648142000	-0.000548000
8	-2.126654000	-1.267688000	0.000138000
6	-4.511767000	-1.531554000	-0.001777000
6	-2.812415000	3.210787000	0.002091000
6	-3.656243000	3.496380000	-1.263377000
6	-3.654733000	3.493930000	1.269129000
6	-1.600866000	4.156902000	0.002252000
6	-5.347533000	-1.228334000	-1.267429000
6	-4.133115000	-3.023047000	-0.002232000
6	-5.349193000	-1.229547000	1.263074000
1	-4.398459000	1.123916000	-0.000311000
1	-3.945271000	4.554153000	-1.284317000
1	-3.083579000	3.285058000	-2.173583000
1	-4.572541000	2.899231000	-1.296062000
1	-3.944149000	4.551552000	1.292261000
1	-4.570709000	2.896293000	1.301936000
1	-3.080804000	3.281265000	2.178227000
1	-1.952150000	5.195377000	0.003824000
1	-0.976039000	4.009463000	0.887854000
1	-0.977611000	4.011700000	-0.884847000
1	-6.235121000	-1.872258000	-1.290467000
1	-5.688140000	-0.188692000	-1.298126000
1	-4.767862000	-1.419611000	-2.177702000
1	-5.044095000	-3.632806000	-0.003233000
1	-3.545878000	-3.286476000	-0.887397000
1	-3.547229000	-3.287362000	0.883561000
1	-6.236776000	-1.873539000	1.284363000
1	-4.770695000	-1.421637000	2.173921000
1	-5.689914000	-0.189958000	1.294285000
78	-0.204142000	-0.353088000	0.000062000
6	1.675745000	0.256955000	-0.000282000
7	0.670437000	-2.181021000	0.000354000
6	2.362400000	1.500740000	-0.001148000
6	3.790191000	1.427046000	-0.000791000
34	4.406555000	-0.399036000	0.000668000
6	2.603528000	-0.894406000	0.000420000
6	2.073454000	-2.181945000	0.000673000
6	2.768821000	-3.422800000	0.001167000
6	2.071056000	-4.606507000	0.001309000
6	0.652760000	-4.573822000	0.000959000
6	0.004684000	-3.346497000	0.000488000
6	4.600330000	2.541031000	-0.001483000
6	4.000730000	3.818190000	-0.002648000
6	2.607411000	3.931029000	-0.003130000
6	1.795508000	2.799279000	-0.002416000
1	3.854691000	-3.413219000	0.001398000
1	2.597885000	-5.555846000	0.001670000
1	0.066871000	-5.485952000	0.001058000
1	-1.075228000	-3.260311000	0.000207000
1	5.682711000	2.447881000	-0.001158000
1	4.627412000	4.705117000	-0.003194000
1	2.147424000	4.915830000	-0.004084000
1	0.718410000	2.881597000	-0.002823000

Table SX. Cartesian coordinates for the **6** complex in the T_1 excited state optimized by the UB3LYP/Lanl2DZ(Pt)/6-31G(d)(C,N,O,Se,H) method.

78	0.284052000	0.378906000	-0.013073000
6	-1.513369000	-0.312187000	-0.057401000
7	-0.735840000	2.120149000	-0.014353000
34	-2.168116000	-2.073297000	-0.110490000
6	-3.923739000	-1.324759000	-0.002366000
6	-2.598786000	0.678435000	-0.011607000
6	-2.153428000	2.021121000	-0.045684000
6	-2.905232000	3.219789000	-0.140691000
6	-2.289653000	4.451001000	-0.150671000
6	-0.870396000	4.510652000	-0.070055000
6	-0.149074000	3.331186000	-0.016306000
1	-3.981416000	3.162164000	-0.236692000
1	-2.877259000	5.359555000	-0.231963000
1	-0.343690000	5.458549000	-0.067358000
1	0.934690000	3.316732000	0.019741000
6	-3.922399000	0.099765000	0.061094000
6	-5.105088000	-2.053032000	0.036571000
6	-6.324875000	-1.377703000	0.156851000
6	-6.351556000	0.017650000	0.252686000
6	-5.167850000	0.748047000	0.210771000
1	-5.216270000	1.823758000	0.320791000
1	-7.298375000	0.536825000	0.368033000
1	-7.251712000	-1.943787000	0.188324000
1	-5.085977000	-3.137402000	-0.018445000
8	1.167583000	-1.470665000	-0.015823000
6	2.429952000	-1.689271000	0.003847000
6	3.444195000	-0.718124000	0.029919000
6	3.302983000	0.683696000	0.040006000
8	2.195281000	1.316154000	0.026035000
6	4.579666000	1.559936000	0.070204000
6	2.824242000	-3.186152000	0.000425000
6	3.697353000	-3.487023000	-1.240257000
6	3.617128000	-3.508397000	1.288913000
6	1.569336000	-4.076780000	-0.047466000
6	5.437050000	1.264752000	-1.182787000
6	4.207062000	3.053144000	0.076868000
6	5.392889000	1.242489000	1.346987000
1	4.458180000	-1.094899000	0.044964000
1	3.953189000	-4.553280000	-1.263591000
1	3.161416000	-3.248287000	-2.165890000
1	4.632961000	-2.918997000	-1.236541000
1	3.875738000	-4.574080000	1.308822000
1	4.548089000	-2.936542000	1.355361000
1	3.021628000	-3.288803000	2.182312000
1	1.871011000	-5.130863000	-0.046152000
1	0.920731000	-3.903207000	0.815957000
1	0.979162000	-3.889536000	-0.949359000
1	6.328012000	1.904524000	-1.183503000
1	5.773026000	0.223718000	-1.217622000
1	4.874890000	1.467829000	-2.101467000
1	5.120584000	3.658924000	0.097753000
1	3.635540000	3.326588000	-0.815334000
1	3.605336000	3.311218000	0.953668000
1	6.282743000	1.882319000	1.390303000
1	4.798742000	1.428981000	2.248900000
1	5.728359000	0.201079000	1.374958000

- 1 A. D. Becke, *J. Chem. Phys.*, 1993, **98**, 5648–5652.
 - 2 P. J. Hay and W. R. Wadt, *J. Chem. Phys.*, 1985, **82**, 270–283.
 - 3 W. J. Hehre, K. Ditchfield and J. A. Pople, *J. Chem. Phys.*, 1972, **56**, 2257–2261.
 - 4 R. Bauernschmitt and R. Ahlrichs, *Chem. Phys. Lett.*, 1996, **256**, 454–464.
 - 5 J. Tomasi, B. Mennucci and R. Cammi, *Chem. Rev.*, 2005, **105**, 2999–3093.
 - 6 F. Wang and T. Ziegler, *J. Chem. Phys.*, , DOI:10.1063/1.2061187.
 - 7 E. Van Lenthe and E. J. Baerends, *J. Comput. Chem.*, 2003, **24**, 1142–1156.
 - 8 P. K. Samanta, D. Kim, V. Coropceanu and J. L. Brédas, *J. Am. Chem. Soc.*, 2017, **139**, 4042–4051.
 - 9 K. Mori, T. P. M. Goumans, E. Van Lenthe and F. Wang, *Phys. Chem. Chem. Phys.*, 2014, **16**, 14523–14530.
 - 10 G. Baryshnikov, B. Minaev and H. Ågren, *Chem. Rev.*, 2017, **117**, 6500–6537.
-